Probing the structure of the HIV-1 Envelope trimer using Aspartate Scanning Mutagenesis

Raksha Das[1], Rohini Datta[1], Raghavan Varadarajan[1,2,*]

[1]Molecular Biophysics Unit, Indian Institute of Science, Bangalore-560012, India

[2]Jawaharlal Nehru Center for Advanced Scientific Research, Bangalore 560 004, India

[*]Corresponding Author

Raghavan Varadarajan, Molecular Biophysics Unit, Indian Institute of Science, Bangalore, 560012 (INDIA), *Email*: varadar@iisc.ac.in, PHONE: +91-80-22932612, FAX: +91-80-23600535

Running Title: Aspartate Scanning mutagenesis of HIV-1 Env trimer

Number of manuscript pages: 51

Number of supplementary material pages: 0

Number of figures: 10

Number of Tables: 2

Abstract:

HIV-1 Env glycoprotein gp160 exists as a trimer of heterodimers on the viral surface. In most structures of the soluble ectodomain of trimeric HIV-1 Envelope glycoprotein, the region from 512-517 of the fusion peptide and 547- 568 of the N- heptad repeat is disordered. We used aspartate scanning mutagenesis of Subtype B, JRFL Env as an alternate method to probe residue burial in the context of cleaved, cell surface expressed Env, as buried residues should be intolerant to substitution with Asp. The data are inconsistent with a fully disordered 547-568 stretch as residues 548, 549, 550, 555, 556, 559, 562, 566-569 are all sensitive to Asp substitution. In the fusion peptide region, residues 513 and 515 were also sensitive to Asp substitution, suggesting that the fusion peptide may not be fully exposed in native Env.gp41 is metastable in the context of native trimer. Introduction of Asp at residues that are exposed in the pre-fusion state but buried in the post-fusion state is expected to destabilize the post-fusion state and any intermediate states where the residue is buried. We therefore performed sCD4 induced gp120 shedding experiments to identify Asp mutants at residues 551, 554-559, 561-567, 569 that could prevent gp120 shedding. We also observed similar mutational effects on shedding for equivalent mutants in the context of Clade C Env from isolate, 4-2J.41. These substitutions can potentially be used to stabilize native like trimer derivatives that are used as HIV-1 vaccine immunogens.

Importance:

In most crystal structures of the soluble ectodomain of the HIV-1 Env trimer, some residues in the fusion and N-heptad repeat regions are disordered. Whether this is true in the context of native, functional Env on the virion surface is not known. This knowledge may be useful for stabilizing Env in its prefusion conformation and will also help to improve understanding of the viral entry process. Burial of the charged

residue Asp in a protein structure is highly destabilizing. We therefore used Asp scanning mutagenesis to probe burial of apparently disordered residues in native Env and, to examine the effect of mutations in these regions on Env stability and conformation as probed by antibody binding to cell surface expressed Env, CD4 induced shedding of HIV-1 gp120, and viral infectivity studies. Mutations that prevent shedding can potentially be used to stabilize native-like Env constructs for use as vaccine immunogens.

Introduction:

HIV-1 is the causative agent of Acquired Immunodeficiency Syndrome (AIDS). The virus infects target cells through its Env glycoprotein. This envelope glycoprotein is synthesized as a gp160 precursor protein inside the cell. During the course of transport to the virion surface, it is cleaved by the host cell protease Furin, into surface exposed gp120 and membrane anchored gp41. The three gp120 and gp41 monomers are associated non-covalently forming a trimer of heterodimers (1, 2). The integrity of this trimer is important for HIV-1 viral entry into the host cell. Since a significant fraction of gp120 is surface exposed, it is the primary target of the host humoral immune response. gp120 binds to the primary host cell receptor CD4, this induces conformational changes in the envelope that in turn expose the co-receptor binding site for binding to CXCR4/CCR5, ultimately leading to virus-cell fusion (1, 3–6).

On the virion surface, there are also other non-functional Env derivatives such as gp41 stumps, and misfolded gp120 termed as junk envelope (7, 8) that elicit non-neutralizing antibodies. Monomeric gp120, when used as a vaccine, also primarily elicits non-neutralizing immune responses (9–11). In order to drive elicitation of broadly protective neutralizing immune responses, the native trimer is thought to be the most relevant immunogen. Many efforts have been made to make an immunogen closely mimics the native trimer. Since gp41 is metastable in nature, a disulfide linkage between gp120 and gp41 in combination with the I559P mutation (SOSIP) has been used to stabilize the trimer (12, 13). In an alternative strategy, the gp120 and gp41 subunits were linked with a G4S 20 residue flexible linker to generate the so called NFL trimer (14–16). A number of other stabilizing mutations have been introduced into these base constructs (17–20) . However, so far none of these derivatives have elicited broadly neutralizing antibodies in animal immunizations (21–24). Challenge studies in rhesus macaques have revealed varying levels of protection against heterologous pathogenic challenge (25, 26). Recently, a cyclically permuted gp120 trimer derived from JRFL sequence was shown to confer significant protection against

heterologous challenge with the same SHIV162.P3 isolate used in the above studies in non-human primates (27). Multiple studies (28–30) have shown that cleaved, cell-surface expressed Env displays some antigenic differences from the BG505 SOSIP.664 soluble gp140 structure that is the template for most immunogen design. A recent single molecule FRET study also suggested that the native, pre-triggered conformation of HIV-1 Env on intact virions, differs subtly from those in the various soluble Env derivatives characterized to date (31–33).

In a previous study, we had shown that aspartate scanning mutagenesis can be a useful tool to probe residue burial in proteins (34) as introduction of Asp at a buried position will significantly destabilize the folded structure. During the course of viral fusion, gp41 undergoes conformational changes in which the NHR (N-heptad repeat) region of gp41 interacts with the CHR (C-heptad repeat) to form a six-helix bundle structure that drives the fusion of viral and host cell membrane. The post-fusion structure of gp41 is known (35). There has been much recent progress in determining the structure of the Env ectodomain gp140 by Cryo-EM and crystallography (36–41) (Figure 1). In most of these structures, the gp41 regions 547-568 and fusion peptide 512-517 are disordered (40). In addition, there is no high-resolution structure of the Env ectodomain, in the absence of any stabilizing ligands or mutations. The prefusion structure of JRFL gp160 (38) suggested that part of the 547-568 region is helical but this needs confirmation by additional experiments. The above structure also involved in a complex with the MAb PGT151, which has recently been suggested to trap Env in a non-native conformation (31). We, therefore mutated individual residues in the above two stretches to aspartate, to probe the burial of residues in these apparently disordered regions. We also substituted a few residues with the bulky hydrophobic residue Tryptophan since this should also perturb the structure when introduced at buried locations (42). In earlier studies, tryptophan scanning mutagenesis has been used to identify membrane facing regions in helical segments of transmembrane proteins (43, 44). We expressed WT and mutated derivatives on the surface of

HEK293T cells and monitored their expression and binding to various antibodies by Flow cytometry (33, 45). To further examine the generality of results obtained with subtype B JRFL Env, a subset of mutations was also made in Env from the Clade C, isolate 4-2J.41, as this isolate is also cleaved and binds selectively to neutralizing antibodies when expressed on the mammalian cell surface (46–48). The data identify sites in both fusion peptide and the 547-568 that are likely to be at least partially buried in native Env.

We were able to identify positions where the Env expression and binding to conformation specific antibodies were not affected by mutation to Asp. During, the course of viral fusion, gp120 is shed, and the N-heptad repeat, and C-heptad repeats of gp41 form a six-helix bundle which drives viral fusion. We therefore also investigated whether these mutations could prevent gp120 shedding and help retain Env glycoprotein in its native, prefusion form, and identified several such mutations that prevent shedding. These mutations can potentially be used to stabilize native-like Env constructs for use as vaccine immunogens.

Results:

Expression of different aspartate mutants

JRFL gp160 (truncated at its cytoplasmic tail: JRFL gp160dCT) when expressed on the HEK 293T cell surface, is efficiently processed into gp120 and gp41, and native-like Env oligomers are displayed on the cell surface (45, 49, 50). Previous studies have shown that cytoplasmic tail truncation has minimal effects on Env conformation (32). Cell surface expressed Env was probed for binding against different neutralizing and non-neutralizing antibodies by FACS. The properly cleaved native-like envelope trimer binds selectively to CD4bs directed neutralizing antibodies such as b12, and significantly less to non-neutralizing antibodies, such as b6 (45). JRFLgp160dCT is truncated at the cytoplasmic tail (residue 711)

for increased surface expression. The gene in the plasmid is not-human codon optimized, so pcTAT plasmid is co-transfected with the Env plasmid into HEK293T cells to enhance expression.

The disordered stretches in the Env crystal structures comprising residues 512-517 (fusion peptide) and 547-568 (HR1) were selected for Asp scanning mutagenesis. Following mutagenesis, individual mutants were transfected into 293T cells. Surface expression was measured by binding of WT and mutants to the 2G12 antibody by FACS as described (28) (Figure 2). Mutants in fusion peptide V513D, G514D and G516D are expressed at lower levels than WT. Although some mutants that lie in the 547-567 region such as G547D, N554D, L555D, A558D, residues 561-566 and T569D are very well expressed suggesting they are likely to be exposed, several residues in this supposedly disordered stretch are sensitive to Asp substitution such as I548D, V549D, L556D. The three residues that do not fall in this disordered region L576, A578, I580 are all buried in published ectodomain structures, (40), and are expectedly sensitive to substitution with Asp residues (Figure 2 and Table 1), validating the approach.

Expression of Tryptophan mutants:

Q567, L568 and A578 were also mutated to Trp to compare with results of Asp substitutions. Q567W has similar expression as wild type, and L568W and A578W have nearly comparable expression (Table 1). A578 is known to be buried in the Env structure (40). The lack of effect seen with the A578W substitution suggests that W is not as good a probe of residue burial as D, confirming the results seen from previous saturation mutagenesis studies (51, 52).

Conformational integrity of mutants:

In addition to native Env, there are other non-native forms of envelope present on the cell surface such as monomeric gp120 and gp41 stumps (13). To examine the conformational integrity of the mutants with

154 respect to the wild-type native-like trimer, cells expressing Env were stained with CD4bs directed
155 neutralizing (b12) and non-neutralizing antibody (b6) for JRFL gp160dCT and VRC01 and F105 for
156 Clade C Env 4-2J.41 (46, 47). Native-like trimeric Env is known to bind better to neutralizing antibodies
157 relative to non-neutralizing ones. 48 hours after transfection, cells were harvested and stained with CD4
158 binding site neutralizing (b12 or VRC01) and non-neutralizing (b6 or F105) antibodies, to screen for an
159 Env which behaves similarly to the wild-type, using already an established FACS method (28, 45, 53).
160 The b12 and b6 binding of all mutants were normalized with respect to wild- type. The b12/b6 ratio
161 provides information on the ability of the unliganded native trimer to adopt a wild-type like conformation
162 as non-native (Figure 3 and Table 1) and cleavage defective forms of Env have been shown previously to
163 have lower b12/ b6 ratios than WT (28, 45, 49).
164 Amongst all the mutants in the fusion peptide 512-517 region, V513D, I515D, have a lower b12/b6 ratio
165 than wild type (Figure 3 and Table 1).The Asp mutants at residues 547, 549, 554, 557, 558, 560, 561,563,
166 565, behaved similarly to the wild-type and apparently did not perturb native trimer formation. However,
167 mutants I548D, L555D, L556D, I559D, Q562D, and residues 566-569 have a lower b12/b6 ratio than
168 wild- type (Table 1). L576D, A578D, I580D mutations also significantly perturb the native trimer
169 conformation and appear to have the highest destabilization amongst all NHR mutants (Figure 3 and Table
170 1). Unlike L568D, A578D; L568W and A578W behaved nearly similar, to wild type. We examined the
171 cleavage efficiency of all mutants expressed on the cell surface by using PGT151 antibody (54, 55) as
172 PGT151 selectively binds to properly formed and cleaved trimers. Almost all mutants were found to be
173 well cleaved on the cell surface (Figure.9). We also examined the effects of a few mutants in the fusion
174 peptide (FP) (V513D, G514D, A517D) and N- heptad repeat (HR1), (Q552D, L555D, Q563D) regions in
175 Clade C Env 4-2J.41. Since this isolate is not neutralized by b12, we could not use b12/b6 ratio to probe
176 the conformational integrity of the cell surface expressed Env. Instead we used the VRC01/F105 ratio

177 since VRC01 and F105 serve as neutralizing and non-neutralizing antibodies for this isolate (47). The
178 values of this ratio for selected Asp mutants in strain 4-2 J.41 are shown in Figure 10.A and the overall
179 trends are similar to those observed for the b12/b6 ratio in corresponding mutants in subtype B JRFL Env
180 (Figure 3).
181
182 **Some mutants diminish gp120 shedding upon treatment with sCD4:**
183 During the course of viral fusion, gp120 binds to the primary host cell receptor (CD4). This leads to
184 conformational changes in gp120 and gp41. gp120 is shed off from the virus and gp41 then drives viral
185 fusion with the host membrane (50, 56). In the post-fusion conformation, the NHR and CHR of gp41 form
186 a six-helix bundle (6HB) structure in which the NHR trimer is surrounded by three CHR helices (Figure
187 1). The mutation V570D has been shown to be 6HB destabilizing using a yeast surface two hybrid display
188 system (57, 58). The same mutation was shown to prevent gp120 shedding using mammalian cell surface
189 display (28). We attempted to identify other gp41 mutations that would prevent shedding since these can
190 be incorporated into Env immunogens to restrict their conformational variability.
191 A few mutations were selected from the NHR of gp41 in the stretch 547- 567, which showed good surface
192 expression and more importantly, a b12/b6 ratio of ≥ 0.7 (Table 1) indicating a WT like conformation. The
193 mutant Env plasmids were co-transfected along with pcTAT plasmid in HEK 293T cells. After 48 hours,
194 the transfected cells were harvested, 1 $X10^6$ cells were incubated with 50µg/ml of sCD4, cells were
195 washed and then incubated with 2G12 at varying concentrations (shown here at 10µg/ml). gp120 shedding
196 from the cell surface was measured by 2G12 binding. The mutants G547D, V549D, Q551D, N553D,
197 N554D, Q560D could not prevent gp120 shedding (Figure 4 and Table 2). However, other mutants
198 namely Q552D, R557D, A558D, A561D, Q563D, R564D, M565D, helped in preventing gp120 shedding
199 (Figure 4 A and Table2). Other mutants that lie in “a” and “d” positions of the NHR post-fusion coiled-

200 coil (35, 57) and also in the apparently in disordered stretch 547-569 in BG505gp140 ectodomain crystal
201 structure (40) were also examined, and these mutants L555D, I559D, Q562D, L566D, T569D prevented
202 gp120 shedding. The previously characterized mutant, V570D was taken as a positive control. All the
203 above mutants behaved in a similar way as V570D (28, 57). Overall, the ability to prevent shedding in the
204 547-570 region is largely restricted to residues in the stretch from 555-570, suggesting that these residues
205 become buried in gp41 intermediates that form during the shedding process (Table 2). We also examined
206 shedding effects in subtype C 4-2J.41 Env. Since this strain is not neutralized by b12, we used VRC01
207 instead. (46–48). Overall, the results for this subtype C Env (Figure. 10B) were similar to those observed
208 with JRFL Env.
209
210 **Mutants that prevent sCD4 induced gp120 shedding showed enhanced recognition of CD4i**
211 **antibodies 17b and 19e with gp41 cluster-I region remain occluded upon sCD4 induction:**
212 Mutants that prevent gp120 shedding upon sCD4 induction may or may not bind to sCD4. To further
213 examine this, cells expressing a subset of mutants shown in Figure 4 were incubated with sCD4 and
214 probed for binding to 17b (1, 59) and 19e (60–62) which bind to CD4i epitopes (Figure 5). Wild type and
215 all the mutants bound to 17b and 19e. The binding MFI for mutants that prevented gp120 shedding
216 (A558D, V570D) increased by more than two-fold after sCD4 induction compared to the mutants that
217 could not prevent gp120 shedding (V549D, Q551D, Q560D). This suggests that mutants that prevent
218 gp120 shedding still bind to sCD4 and this results in exposure of CD4i epitopes (Figure 5 A, B). D49
219 antibody binds to the gp41 cluster-1 region that is normally exposed upon gp120 shedding (28, 63, 64).
220 Expectedly, following incubation with sCD4, mutants which prevent gp120 shedding do not show any
221 increased binding to D49, in contrast to what is observed for mutants that do not prevent shedding (Figure
222 5.C).

Pseudoviral Infectivity of all Asp mutants:

The infectivity of all the JRFL Asp mutants was measured. Pseudoviruses were produced from HEK-293T cells. Equivalent p24 levels of WT and all the mutants were used to infect TZMbl cells. The effects of Asp mutations on cell surface Env probe the corresponding residue burial in the context of a native-like trimer. In contrast, effects on pseudoviral infectivity probe burial at all stages of the infection process. All the mutants that prevented gp120 shedding were found to be non-infectious (Figure 6, Tables 1-2). This might be because either shedding is a pre-requisite for downstream steps that lead to fusion, or the mutations prevent formation of a crucial intermediate in the fusion process. However, some of the mutants that did not prevent gp120 shedding like those at 548, 549, were also found to be non-infectious likely because these residues are buried in the post-fusion structure (Table 2). In the fusion peptide region, 513, 514 and 517 show the largest decreases in infectivity, whereas 512, 515 and 516 are relatively unaffected. This is a surprising result, suggesting that the entire fusion peptide is not buried during various stages of the fusion process. Overall, Asp mutations have stronger effects on infectivity than previously observed for Ala mutants (65) at most positions, consistent with the greater burial penalty of Asp versus Ala.

Discussion:

In case of HIV-1 Env, both structures of the post fusion six helix bundle (35) and more recently, crystal structures of gp140 ectodomain constructs are available (37, 38, 40, 41) (Figure 1). The latter are thought to closely resemble the native, prefusion conformation of the Env ectodomain on the virion. In most prefusion structures, there is missing electron density between residues 512-517 of the fusion peptide and the N-heptad repeat stretch from residues 547-568 (Figure 1). All existing structures were stabilized by MAbs and engineered disulfides and most contain an I559P mutation. There is currently no structure of

native, unliganded Env. In addition, recent single molecule FRET experiments suggest that native Env as it exists on the virion, may have a conformation subtly different from that seen in existing structures of soluble gp140 ectodomains (31). Hence, we have used aspartate scanning mutagenesis as an alternate approach to probe residue burial in these apparently disordered regions, in the context of viral Env expressed on the mammalian cell surface. It is known that aspartate, being a charged residue, is destabilizing and poorly tolerated at buried positions, and conversely, is well tolerated at exposed non-active site residues (34) with the obvious exception of a disulfide bonded Cys residue. Hence, Asp scanning mutagenesis can be used to probe residue burial. We also mutated a few residues with tryptophan to probe the effect of a bulkier, hydrophobic group on conformation and function (42, 66).

We introduced Asp mutations at a number of non-Cys positions in an Env expressing plasmid with a cytoplasmic tail truncation (JRFLgp160dCT) as well as a subset of these mutations in Env from the Clade C Env from isolate 4-2J.41. The JRFLgp160dCT bearing mutations were co-transfected with pcTAT plasmid into HEK293T cells. After 48 hours of transfection, cells were harvested and probed with monoclonal antibody 2G12 for surface expression, and with MAbs b12 and b6 for Clade B, JRFL strain and VRC01 and F105 for Clade C, 4-2 J.41 to assess conformational integrity compared to wild- type. A few of the mutants had very minimal expression on the cell surface namely L556D, L576D, A578D, and I580D (Figure 2 and Table 1). These mutations also had an impact on the native conformation of Env. The b12/b6 ratio was lowest for L576D, A578D, and I580D (Figure 3). These three residues acted as a positive control for method validation, since they are known to be buried in the gp140ectodomain structure (40) .Other mutants such as V513D, I515D in the fusion peptide and numerous residues in the 547-570 stretch show significant perturbations in expression and/or conformation, relative to WT. These observations suggest that the fusion peptide is not fully exposed and that the 547-568 stretch is not disordered in native, membrane bound Env. A cryo-EM structure of a soluble B41SOSIP ectodomain trimer reveals that the

fusion peptide becomes ordered upon b12 binding (41). In this structure residues 513 and 516 are partially buried consistent with the reduced b12/b6 ratio as seen for Asp substitutions at these positions. The same residues also show reduced surface expression in the absence of b12, indicating they are partially buried in unliganded Env as well (Figure 3 and Table1). gp41 of Env glycoprotein is metastable in nature. The accessibility values of these residues in a recent Cryo-EM structure of JRFL gp160dCT in complex with PGT151 were taken for comparison (38). The structure is in complex with PGT151, the stoichiometry of PGT151 to trimer is 2:1, *i.e.* 2Fabs bind per trimer. Hence, the interfaces of all the protomers are not equivalent, which is clearly evident from Table 2. Further, a recent FRET study (31) suggests that PGT151 may trap Env in a conformation different from the predominant 'state 1' conformation present on the virion. The Env structure is highly dynamic and depending on the conformation, the fusion peptide may be either exposed or sequestered in the trimeric core on native Env on the virion surface (41, 67). In the closed HIV-1 ectodomain structures, the fusion peptide is often found to be disordered (68, 69). The fusion peptide specific antibody VRC34 binds to the prefusion trimer contacting the heavy chain at residues 517, 519 and 520. From mutational antigenic profiling studies, it was shown that escape variants are located primarily in the stretch from 512-518, of which Asp at 514 and 516 were escape variants (68, 70–72). Interestingly, many viral strains show partial neutralization by VRC34 (68). This is consistent with the fusion peptide having multiple conformations with varying degrees of exposure on native Env. Asp substitutions at positions 512, 515, 516 show relatively small decrease in infectivity while those at 513, 514 and 517 show large decreases. This periodicity may be indicative of an amphiphilic helical structure of this stretch during fusion. In two Ala mutagenesis studies (65, 73), some mutants in the 547-567 stretch were reported to have folding and association defects, consistent with our results (Table 1). Compared to aspartate mutations at 568 and 578, tryptophan mutations at A578 and L568 have

291 comparable expression and b12/b6 ratio to wild type confirming that D is superior to W in probing residue
292 burial (Table 1).
293 The trimerization of Env is largely mediated by gp41 and assisted by the V1V2 loop of gp120 (39). gp120
294 sheds off during the course of viral fusion. We examined if Asp mutants that behaved like wild- type in
295 terms of surface expression and b12/b6 ratio could prevent sCD4 induced gp120 shedding. Mutants which
296 prevented shedding were largely found in the 555-566 residue stretch (Figure 4 and Table 2). It is believed
297 the mutations that are able to prevent gp120 shedding (28, 74–76) destabilize the formation of the six-
298 helix bundle (6HB) or other fusion intermediate conformations. However, it might also be possible that
299 such mutants prevent binding to sCD4. In the sCD4 bound trimer structure, the co-ordinates for the above
300 mentioned NHR residues are missing and V570D has an accessibility of 61% (PDB ID- 5U1F) (77).
301 Hence, it is unlikely that these mutations prevent CD4 binding, instead, it is more likely that they prevent
302 subsequent conformational changes that result in shedding. To further probe whether such mutants bind
303 to sCD4, sCD4 induced binding to antibodies 17b and 19e, which bind to CD4 induced epitopes was
304 monitored. Mutants that prevented shedding showed increased binding to 17b and 19e in the presence of
305 CD4 relative to WT (1, 59, 61, 78).This is likely because gp120 is not shed off, but also confirm that these
306 mutants are indeed competent to bind CD4. Further, the mutants that prevent gp120 shedding do not show
307 any increment in binding to D49, an antibody that binds to the cluster-1 region which gets exposed after
308 gp120 shedding (63, 64). In contrast, enhanced D49 recognition is seen for mutants that do not prevent
309 shedding as gp120 is shed off and the epitope is exposed for binding (Figure.5.C).
310 No correlation with ability to prevent shedding was seen with either location in the helical wheel or
311 accessibility in the post fusion structure (Table 2, Figure 7). The residues that prevent gp120 shedding are
312 not found to be more conserved than residues that do not prevent shedding (Figure 8). The data suggest
313 that each residue in the 555-566 stretch is likely to be largely buried in one or more of the intermediates

on the fusion pathway, consequently Asp mutations in this stretch, destabilize such intermediates relative to the native state. Such mutations may therefore stabilize the trimer in the prefusion conformation. The mutants L555D, I559D, Q562D, L566D, T569D, L576D, I580D are also not infective which is consistent with their positions in the NHR post-fusion structure (Figure 6) as all of them lie in "a" and "d" position of the NHR coiled-coil and are buried in the post-fusion conformation (35, 65). Overall, the reduced infectivity of Asp mutants either occur at positions that prevent shedding, or those that are buried in the post-fusion structure. This in turn suggests that all Asp mutants that prevent shedding occur at positions that are buried at some stage in the fusion process. A small subset of Asp mutants was made in Clade C 4-2J.41 Env. The overall results were very similar to those observed for corresponding positions in Clade B JRFL Env (Figure 3, 4, 10).

Proline mutations at L555, I559, L566, T569, I573, V580 were previously made in SOS gp140 to understand the effect of proline as it is known to cause a kink in a helix and can therefore be useful to probe helicity. L555P expressed poorly. I559P, I573P, V580P have expression comparable to wild-type (76). In the same study (76), the effect of mutating residues near position 559 in JRFL SOSgp140was addressed. L556P, R557P, A558P, I559P, M565P have similar expression as the wild-type Mutations E560P, A561P, Q562P, Q563P, R564P have higher expression than wild-type. Residues in this apparently disordered stretch were further mutated to Proline in BG505and C16055 Env(20) and it was found that S553P, N554P, L555P, Q562P, Q563P bound better to trimer specific bNAbs than non-neutralizing antibodies. L555P has increased yield and more ordered trimers than wild type. The accessibility of residues probed by our experimental method correlates only moderately with the accessibilities in the recent Cryo-EM structure of JRFL gp160dCT at most positions (38). For example, residues 555, 566, 567 are positions at which at least one residue in the protomer has an accessibility <10%, are sensitive to Asp substitution (Figure 3). However, several residues (Figure 3) that are sensitive to Asp substitution, such as

548, 556, 564, 570 are exposed in all protomers and conversely some apparently buried residues (562, 570) are relatively insensitive to mutation. In the existing ectodomain structures, a proline in this region of the protein is present. While it is possible, that this might be responsible for the apparent disorderedness of this stretch (79), this is unlikely because there are several studies that show Pro can be incorporated even in helical stretches without much structural rearrangement and at moderate energetic cost (80–83). In summary, using Asp scanning mutagenesis, we have probed residue burial in two apparently disordered stretches. The data identify sites in both regions that are likely to be buried in native Env in the virion context. The data suggest that residues in the 555-566 stretch are likely to be buried in one or more fusion intermediates. Asp substitutions that prevent shedding without affecting expression or b12/b6 binding ratios can potentially be used to stabilize Env in native-like conformations for structural studies and vaccine applications.

360

361

362

363

364

365

366

367 **Materials and Methods:**

368 **Cell lines and antibodies:** HEK 293T cells were used for mammalian cell surface expression. These cells
369 are grown in DMEM 10%FBS and 1% antibiotics (Penicillin-Streptomycin and Amphotericin). TZMbL is
370 an engineered Hela cell line that expresses CD4 and CXCR4 receptors and is grown in same media as
371 described above. MAb 2G12 is used to probe surface expression. MAbs b12 and b6 are used for
372 determining conformational integrity of cell surface expressed Env, JRFL gp160dCT, VRCO1 and F105
373 are used for 4-2J.41 Env (47). sCD4 is used for the shedding experiment.

374

375 **Constructs:** pSVIII JRFL gp160dCT expression plasmid (45) was used for cell surface expression of
376 JRFLgp160dCT and mutations were incorporated by site directed mutagenesis. HXBC2 numbering was
377 followed and mutations were confirmed with DNA sequencing. JRFL gp160 dCT has a cytoplasmic tail
378 truncation at residue 711 and the Env gene present is non- human codon optimized viral sequence. Hence
379 pcTAT, that codes for HIV-1 tat protein, is transfected along with the psVIII expression plasmid. A subset
380 of mutants were made in the context of Clade C Env 4-2J.41 and probed using cell surface expression to
381 see if the effects are strain specific (47).

382

Transient Transfection of Env plasmid into HEK 293T cells: One day prior to transfection, 3 X 10^6 293T cells were seeded in a T75 culture flask. After 24 hours, the cells were transfected with pSVIII JRFLgp160dCT and 4-2J.41 Env expression plasmids encoding Env (Wt and mutants) and pcTAT in a ratio of 4:1. The transfection mixture was prepared in serum free media with DNA:PEI in a ratio of 1:4. The transfection mixture was incubated for 10minutes. After incubation, serum containing medium was added and the mixture was added into the flask containing 293T cells.

Staining of surface expressed Env for FACS analysis: After 48 hours of transfection, the cells were harvested with PBS containing 5mM EDTA and washed with FACS buffer (PBS, 5% FBS and 0.02% azide). The harvested cells (4X10^5 cells per tube) were stained with the desired antibody for 1hr at 4˚C. The antibody-cell mixture was washed with FACS buffer (PBS pH7.4, 5% fetal bovine serum and 0.02% azide).Anti-human IgG phycoerythrin (PE) (Sigma) at a 1:100 dilution was added and incubated for 1 hour at 4˚C, followed by a wash with FACS buffer (45). The stained cells were analyzed on a FACS analyzer (BD Accuri). On FSC-SSC plots, the cells were gated to discriminate between dead cells, doublets and live or single cells. The MFI values were obtained from the gated single cell population. In each experiment, unstained controls, secondary antibody controls and untransfected cells with primary antibody controls were prepared at the same time as test samples. Each FACS experiment was repeated independently (with independent transfection experiments) to check for consistency of results. BD-Accuri software was used to analyze the data.

sCD4 induced gp120 shedding experiment: 48 hours after transfection, cells were harvested and washed with FACS buffer. Harvested cells (1 X 10^6 cells per tube) were incubated with or without sCD4 at 50 µg/ml concentration for 2 hours at 4˚C with occasional mixing. To remove shedgp120, cells were washed

406 with FACS buffer. Cells were then incubated with 2G12 or VRC01 antibody at various concentrations
407 (shown here are 10µg/ml of 2G12 and 30µg/ml of VRC01 for JRFL gp160dCT and 4-2J.41 Env
408 respectively) (47) for 1 hour at 4˚C. After a wash, cells were incubated with anti-human IgG-PE (Sigma)
409 to stain 2G12 and VRC01 antibody bound cells. After a wash, cells were analyzed on a FACS analyzer
410 (BD-Accuri). BD-Accuri software was used to analyze the data (28).
411
412 **Pseudoviral generation and infectivity assay:** HEK 293T cells were transfected with a plasmid
413 containing virus backbone lacking the Env gene (pSG3Δenv) and a mutant Env plasmid (pSVIII JRFL
414 gp160dCT) in 1:3 ratio using PEI (Cat.no.23966, Polysciences, USA). After 48hours of transfection, the
415 supernatant was collected and stored at -80°C. For testing infectivity, the viral dilutions were mixed with
416 10,000 TZM-bl cells plated in a 96 well flat bottom plate and incubated at 37°C for 48hours (84–88).
417 After incubation, 100µl of media was removed from each well and 80µl of Britelite plus reagent (Perkin
418 Elmer) was added. After 2 minutes of incubation at room temperature, cells were lysed by gentle
419 pipetting. The 100µl volume of lysed cells was transferred into a black plate and luminescence was
420 measured in a Luminometer Victor X2 (Perkin Elmer). The infectivity was plotted in relative
421 luminescence units (RLUs).
422
423 **sCD4 induced gp120 binding to 17b, 19e and D49**: 48 hours after transfection, cells were harvested and
424 washed with FACS buffer. Harvested cells (1 X 10^6 cells per tube) were incubated with or without sCD4
425 at 50 µg/ml concentration for 2 hours at 4˚C with occasional mixing. To remove shedgp120, cells were
426 washed with FACS buffer. Cells were then incubated with 17b 19e and D49 antibody at 10 µg/ml for 1
427 hour at 4˚C. After a wash, cells were incubated with anti-human IgG-PE (Sigma) to stain 2G12 antibody

bound cells. After a wash, cells were analyzed on a FACS analyzer (BD-Accuri). BD-Accuri software was used to analyze the data (28).

Acknowledgements:

We thank R.Wyatt for pSVIII-JRFL gp160 and pcTAT plasmid, the Neutralizing Antibody Consortium of IAVI and the NIH AIDS Research and Reference Program for various HIV-1 directed monoclonal antibodies. This work was funded by the International Aids Vaccine Initiative grant (grant number COATOD00107) and a grant from National Institutes of Health (grant number R01AI118366-01, DT.15/7/2015) to RV. We also acknowledge funding for infrastructural support from the following programs of the Government of India: DST-FIST, UGC Center for Advanced Study, the DBT-IISc Partnership Program, and of a JC Bose Fellowship from DST to RV. We thank Dr. Jayanta Bhattacharya and Dr. Supratik Das for kindly providing us the Clade C Env 4-2J.41 plasmid. We thank Dr. Ujjwal Rathore, Dr. Sannula Keshavardhana and RV lab members for their valuable suggestions.

Author Contributions

R.V. and R.D. designed the experiments. R.D. performed all the experiments except for mutations at positions 567, 568 and 578 (carried out by R.Da). R.V. and R.D. analyzed the overall data and wrote most of the manuscript with critical inputs and review from all other authors.

References:

1. Kwong PD, Wyatt R, Robinson J, Sweet RW, Sodroski J, Hendrickson WA. 1998. Structure of an HIV gp120 envelope glycoprotein in complex with the CD4 receptor and a neutralizing human antibody. Nature 393:648–659.

2. Pantophlet R, Burton DR. 2006. GP120: target for neutralizing HIV-1 antibodies. Annu Rev Immunol 24:739–769.

3. Clapham PR, Weiss RA. 1997. Immunodeficiency viruses. Spoilt for choice of co-receptors. Nature 388:230–231.

4. Dalgleish AG, Beverley PC, Clapham PR, Crawford DH, Greaves MF, Weiss RA. 1984. The CD4 (T4) antigen is an essential component of the receptor for the AIDS retrovirus. Nature 312:763–767.

5. Doms RW. 2000. Beyond receptor expression: the influence of receptor conformation, density, and affinity in HIV-1 infection. Virology 276:229–237.

6. Graham BS, Wright PF. 1995. Candidate AIDS vaccines. N Engl J Med 333:1331–1339.

7. Crooks ET, Tong T, Osawa K, Binley JM. 2011. Enzyme digests eliminate nonfunctional Env from HIV-1 particle surfaces, leaving native Env trimers intact and viral infectivity unaffected. J Virol 85:5825–5839.

8. Tong T, Crooks ET, Osawa K, Binley JM. 2012. HIV-1 virus-like particles bearing pure env trimers expose neutralizing epitopes but occlude nonneutralizing epitopes. J Virol 86:3574–3587.

9. Rerks-Ngarm S, Pitisuttithum P, Nitayaphan S, Kaewkungwal J, Chiu J, Paris R, Premsri N, Namwat C, de Souza M, Adams E, Benenson M, Gurunathan S, Tartaglia J, McNeil JG, Francis DP, Stablein D, Birx DL, Chunsuttiwat S, Khamboonruang C, Thongcharoen P, Robb ML, Michael NL, Kunasol P, Kim JH, MOPH-TAVEG Investigators. 2009. Vaccination with ALVAC and AIDSVAX to prevent HIV-1 infection in Thailand. N Engl J Med 361:2209–20.

10. Haynes BF, Gilbert PB, McElrath MJ, Zolla-Pazner S, Tomaras GD, Alam SM, Evans DT, Montefiori DC, Karnasuta C, Sutthent R, Liao H-X, DeVico AL, Lewis GK, Williams C, Pinter A, Fong Y, Janes H, DeCamp A, Huang Y, Rao M, Billings E, Karasavvas N, Robb ML, Ngauy V, de Souza MS, Paris R, Ferrari G, Bailer RT, Soderberg KA, Andrews C, Berman PW, Frahm N, De Rosa SC, Alpert MD, Yates NL, Shen X, Koup RA, Pitisuttithum P, Kaewkungwal J, Nitayaphan S, Rerks-Ngarm S, Michael NL, Kim JH. 2012. Immune-Correlates Analysis of an HIV-1 Vaccine Efficacy Trial. N Engl J Med 366:1275–1286.

11. Johnston MI, Fauci AS. 2007. An HIV Vaccine — Evolving Concepts. N Engl J Med 356:2073–2081.

12. Beddows S, Schulke N, Kirschner M, Barnes K, Franti M, Michael E, Ketas T, Sanders RW,

493 Maddon PJ, Olson WC, Moore JP. 2005. Evaluating the immunogenicity of a disulfide-stabilized,
494 cleaved, trimeric form of the envelope glycoprotein complex of human immunodeficiency virus
495 type 1. J Virol 79:8812–8827.

496 13. Binley JM, Sanders RW, Master A, Cayanan CS, Wiley CL, Schiffner L, Travis B, Kuhmann S,
497 Burton DR, Hu SL, Olson WC, Moore JP. 2002. Enhancing the proteolytic maturation of human
498 immunodeficiency virus type 1 envelope glycoproteins. J Virol 76:2606–2616.

499 14. Kovacs JM, Noeldeke E, Ha HJ, Peng H, Rits-Volloch S, Harrison SC, Chen B. 2014. Stable,
500 uncleaved HIV-1 envelope glycoprotein gp140 forms a tightly folded trimer with a native-like
501 structure. Proc Natl Acad Sci 111:18542–18547.

502 15. Sharma SK, deVal N, Bale S, Guenaga J, Tran K, Feng Y, Dubrovskaya V, Ward AB, Wyatt RT.
503 2015. Cleavage-Independent HIV-1 Env Trimers Engineered as Soluble Native Spike Mimetics for
504 Vaccine Design. Cell Rep 11:539–550.

505 16. Sanders RW, Moore JP. 2017. Native-like Env trimers as a platform for HIV-1 vaccine design.
506 Immunol Rev 275:161-182.

507 17. De Taeye SW, Ozorowski G, Torrents De La Peña A, Guttman M, Julien JP, Van Den Kerkhof
508 TLGM, Burger JA, Pritchard LK, Pugach P, Yasmeen A, Crampton J, Hu J, Bontjer I, Torres JL,
509 Arendt H, Destefano J, Koff WC, Schuitemaker H, Eggink D, Berkhout B, Dean H, Labranche C,
510 Crotty S, Crispin M, Montefiori DC, Klasse PJ, Lee KK, Moore JP, Wilson IA, Ward AB, Sanders
511 RW. 2015. Immunogenicity of Stabilized HIV-1 Envelope Trimers with Reduced Exposure of Non-
512 neutralizing Epitopes. Cell 163:1702–1715.

513 18. Zhang P, Gorman J, Geng H, Liu Q, Lin Y, Tsybovsky Y, Go EP, Dey B, Andine T, Kwon A, Patel

514 M, Gururani D, Uddin F, Guzzo C, Cimbro R, Miao H, McKee K, Chuang GY, Martin L, Sironi F,
515 Malnati MS, Desaire H, Berger EA, Mascola JR, Dolan MA, Kwong PD, Lusso P. 2018.
516 Interdomain Stabilization Impairs CD4 Binding and Improves Immunogenicity of the HIV-1
517 Envelope Trimer. Cell Host Microbe 23:832–844.e6.

518 19. Kulp DW, Steichen JM, Pauthner M, Hu X, Schiffner T, Liguori A, Cottrell CA, Havenar-
519 Daughton C, Ozorowski G, Georgeson E, Kalyuzhniy O, Willis JR, Kubitz M, Adachi Y, Reiss
520 SM, Shin M, De Val N, Ward AB, Crotty S, Burton DR, Schief WR. 2017. Structure-based design
521 of native-like HIV-1 envelope trimers to silence non-neutralizing epitopes and eliminate CD4
522 binding. Nat Commun 8:1655.

523 20. Yang L, Sharma SK, Cottrell C, Guenaga J, Tran K, Wilson R, Behrens AJ, Crispin M, de Val N,
524 Wyatt RT. 2018. Structure-guided redesign improves NFL HIV Env Trimer integrity and identifies
525 an inter-protomer disulfide permitting post-expression cleavage. Front Immunol 9:1631.

526 21. Moore JP. 2014. Native-like BG505 SOSIP.664 Trimers Induce Autologous Tier-2 NAbs against
527 Complex Epitopes in Rabbits and Macaques. AIDS Res Hum Retroviruses 30:A67–A67.

528 22. Sanders RW, Van Gils MJ, Derking R, Sok D, Ketas TJ, Burger JA, Ozorowski G, Cupo A,
529 Simonich C, Goo L, Arendt H, Kim HJ, Lee JH, Pugach P, Williams M, Debnath G, Moldt B, Van
530 Breemen MJ, Isik G, Medina-Ramírez M, Back JW, Koff WC, Julien JP, Rakasz EG, Seaman MS,
531 Guttman M, Lee KK, Klasse PJ, LaBranche C, Schief WR, Wilson IA, Overbaugh J, Burton DR,
532 Ward AB, Montefiori DC, Dean H, Moore JP. 2015. HIV-1 neutralizing antibodies induced by
533 native-like envelope trimers. Science 349.aac4223.

534 23. Torrents de la Peña A, Julien JP, de Taeye SW, Garces F, Guttman M, Ozorowski G, Pritchard LK,
535 Behrens AJ, Go EP, Burger JA, Schermer EE, Sliepen K, Ketas TJ, Pugach P, Yasmeen A, Cottrell

CA, Torres JL, Vavourakis CD, van Gils MJ, LaBranche C, Montefiori DC, Desaire H, Crispin M, Klasse PJ, Lee KK, Moore JP, Ward AB, Wilson IA, Sanders RW. 2017. Improving the Immunogenicity of Native-like HIV-1 Envelope Trimers by Hyperstabilization. Cell Rep 20:1805–1817.

24. Ringe RP, Ozorowski G, Rantalainen K, Struwe WB, Matthews K, Torres JL, Yasmeen A, Cottrell CA, Ketas TJ, LaBranche CC, Montefiori DC, Cupo A, Crispin M, Wilson IA, Ward AB, Sanders RW, Klasse PJ, Moore JP. 2017. Reducing V3 Antigenicity and Immunogenicity on Soluble, Native-Like HIV-1 Env SOSIP Trimers. J Virol 91:e00677-17.

25. Barouch DH, Stephenson KE, Borducchi EN, Smith K, Stanley K, McNally AG, Liu J, Abbink P, Maxfield LF, Seaman MS, Dugast AS, Alter G, Ferguson M, Li W, Earl PL, Moss B, Giorgi EE, Szinger JJ, Eller LA, Billings EA, Rao M, Tovanabutra S, Sanders-Buell E, Weijtens M, Pau MG, Schuitemaker H, Robb ML, Kim JH, Korber BT, Michael NL. 2013. XProtective efficacy of a global HIV-1 mosaic vaccine against heterologous SHIV challenges in rhesus monkeys. Cell 155:531.

26. Saunders KO, Santra S, Parks R, Yates NL, Sutherland LL, Scearce RM, Balachandran H, Bradley T, Goodman D, Eaton A, Stanfield-Oakley SA, Tartaglia J, Phogat S, Pantaleo G, Esteban M, Gomez CE, Perdiguero B, Jacobs B, Kibler K, Korber B, Montefiori DC, Ferrari G, Vandergrift N, Liao H-X, Tomaras GD, Haynes BF. 2018. Immunogenicity of NYVAC Prime-Protein Boost Human Immunodeficiency Virus Type 1 Envelope Vaccination and Simian-Human Immunodeficiency Virus Challenge of Nonhuman Primates. J Virol 92:e02035-17.

27. Jones AT, Shen X, Walter KL, LaBranche CC, Wyatt LS, Tomaras GD, Montefiori DC, Moss B, Barouch DH, Clements JD, Kozlowski PA, Varadarajan R, Amara RR. 2019. HIV-1 vaccination by

needle-free oral injection induces strong mucosal immunity and protects against SHIV challenge. Nat Commun 10:798.

28. Kesavardhana S, Varadarajan R. 2014. Stabilizing the native trimer of HIV-1 Env by destabilizing the heterodimeric interface of the gp41 postfusion six-helix bundle. J Virol 88:9590–9604.

29. Alsahafi N, Anand SP, Castillo-Menendez L, Verly MM, Medjahed H, Prévost J, Herschhorn A, Richard J, Schön A, Melillo B, Freire E, Smith AB, Sodroski J, Finzi A. 2018. SOSIP Changes Affect Human Immunodeficiency Virus Type 1 Envelope Glycoprotein Conformation and CD4 Engagement. J Virol 92:e01080-1818.

30. Castillo-Menendez LR, Nguyen HT, Sodroski J. 2018. Conformational Differences between Functional Human Immunodeficiency Virus Envelope Glycoprotein Trimers and Stabilized Soluble Trimers. J Virol 93:e01709-18.

31. Lu M, Ma X, Castillo-Menendez LR, Gorman J, Alsahafi N, Ermel U, Terry DS, Chambers M, Peng D, Zhang B, Zhou T, Reichard N, Wang K, Grover JR, Carman BP, Gardner MR, Nikić-Spiegel I, Sugawara A, Arthos J, Lemke EA, Smith AB, Farzan M, Abrams C, Munro JB, McDermott AB, Finzi A, Kwong PD, Blanchard SC, Sodroski JG, Mothes W. 2019. Associating HIV-1 envelope glycoprotein structures with states on the virus observed by smFRET. Nature 568:415-419.

32. Castillo-Menendez LR, Witt K, Espy N, Princiotto A, Madani N, Pacheco B, Finzi A, Sodroski J. 2018. Comparison of Uncleaved and Mature Human Immunodeficiency Virus Membrane Envelope Glycoprotein Trimers. J Virol 92:e00277-18.

33. Lebeda FJ, Adler M, Dembek ZF. 2018. Yesterday and today: The impact of research conducted at

camp detrick on botulinum toxin. Mil Med 183:85-95.

34. Bajaj K, Chakrabarti P, Varadarajan R. 2005. Mutagenesis-based definitions and probes of residue burial in proteins. Proc Natl Acad Sci U S A 102:16221–16226.

35. Chan DC, Fass D, Berger JM, Kim PS. 1997. Core structure of gp41 from the HIV envelope glycoprotein. Cell 89:263–273.

36. Bartesaghi A, Merk A, Borgnia MJ, Milne JL, Subramaniam S. 2013. Prefusion structure of trimeric HIV-1 envelope glycoprotein determined by cryo-electron microscopy. Nat Struct Mol Biol 20:1352–1357.

37. Julien JP, Cupo A, Sok D, Stanfield RL, Lyumkis D, Deller MC, Klasse PJ, Burton DR, Sanders RW, Moore JP, Ward AB, Wilson IA. 2013. Crystal structure of a soluble cleaved HIV-1 envelope trimer. Science 342:1477–1483.

38. Lee JH, Ozorowski G, Ward AB. 2016. Cryo-EM structure of a native, fully glycosylated, cleaved HIV-1 envelope trimer. Science 351:1043–1048.

39. Lyumkis D, Julien JP, de Val N, Cupo A, Potter CS, Klasse PJ, Burton DR, Sanders RW, Moore JP, Carragher B, Wilson IA, Ward AB. 2013. Cryo-EM structure of a fully glycosylated soluble cleaved HIV-1 envelope trimer. Science 342:1484–1490.

40. Pancera M, Zhou T, Druz A, Georgiev IS, Soto C, Gorman J, Huang J, Acharya P, Chuang GY, Ofek G, Stewart-Jones GB, Stuckey J, Bailer RT, Joyce MG, Louder MK, Tumba N, Yang Y, Zhang B, Cohen MS, Haynes BF, Mascola JR, Morris L, Munro JB, Blanchard SC, Mothes W, Connors M, Kwong PD. 2014. Structure and immune recognition of trimeric pre-fusion HIV-1 Env. Nature 514:455–461.

600 41. Ozorowski G, Pallesen J, De Val N, Lyumkis D, Cottrell CA, Torres JL, Copps J, Stanfield RL,
601 Cupo A, Pugach P, Moore JP, Wilson IA, Ward AB. 2017. Open and closed structures reveal
602 allostery and pliability in the HIV-1 envelope spike. Nature 547:360–361.

603 42. Sharp LL, Zhou J, Blair DF. 1995. Tryptophan-Scanning Mutagenesis of MotB, an Integral
604 Membrane Protein Essential for Flagellar Rotation in Escherichia coli. Biochemistry 34:9166–
605 9171.

606 43. Caballero-Rivera D, Cruz-Nieves OA, Oyola-Cintrón J, Torres-Núñez DA, Otero-Cruz JD,
607 Lasalde-Dominicci JA. 2012. Tryptophan scanning mutagenesis reveals distortions in the helical
608 structure of the δM4 transmembrane domain of the Torpedo californica nicotinic acetylcholine
609 receptor. Channels 6:111-23.

610 44. Sharp LL, Zhou J, Blair DF. 2006. Features of MotA proton channel structure revealed by
611 tryptophan-scanning mutagenesis. Proc Natl Acad Sci 92:7946–7950.

612 45. Pancera M, Wyatt R. 2005. Selective recognition of oligomeric HIV-1 primary isolate envelope
613 glycoproteins by potently neutralizing ligands requires efficient precursor cleavage. Virology
614 332:145–156.

615 46. Ringe R, Thakar M, Bhattacharya J. 2010. Variations in autologous neutralization and CD4
616 dependence of b12 resistant HIV-1 clade C env clones obtained at different time points from
617 antiretroviral naïve Indian patients with recent infection. Retrovirology 7:76.

618 47. Boliar S, Das S, Bansal M, Shukla BN, Patil S, Shrivastava T, Samal S, Goswami S, King CR,
619 Bhattacharya J, Chakrabarti BK. 2015. An efficiently cleaved HIV-1 clade C Env selectively binds
620 to neutralizing antibodies. PLoS One 10:e0122443.

621 48. Das S, Boliar S, Samal S, Ahmed S, Shrivastava T, Shukla BN, Goswami S, Bansal M, Chakrabarti
622 BK. 2017. Identification and characterization of a naturally occurring, efficiently cleaved,
623 membrane-bound, clade A HIV-1 Env, suitable for immunogen design, with properties comparable
624 to membrane-bound BG505. Virology 510:22–28.

625 49. Chakrabarti BK, Pancera M, Phogat S, O'Dell S, McKee K, Guenaga J, Robinson J, Mascola J,
626 Wyatt RT. 2011. HIV type 1 Env precursor cleavage state affects recognition by both neutralizing
627 and nonneutralizing gp41 antibodies. AIDS Res Hum Retroviruses 27:877–887.

628 50. Moore JP, McKeating JA, Weiss RA, Sattentau QJ. 1990. Dissociation of gp120 from HIV-1
629 virions induced by soluble CD4. Science 250:1139–1142.

630 51. Tripathi A, Gupta K, Khare S, Jain PC, Patel S, Kumar P, Pulianmackal AJ, Aghera N, Varadarajan
631 R. 2016. Molecular Determinants of Mutant Phenotypes, Inferred from Saturation Mutagenesis
632 Data. Mol Biol Evol 33:2960–2975.

633 52. Haddox HK, Dingens AS, Bloom JD. 2016. Experimental Estimation of the Effects of All Amino-
634 Acid Mutations to HIV's Envelope Protein on Viral Replication in Cell Culture. PLoS Pathog
635 12:e1006114.

636 53. Grundner C, Mirzabekov T, Sodroski J, Wyatt R. 2002. Solid-phase proteoliposomes containing
637 human immunodeficiency virus envelope glycoproteins. J Virol 76:3511–3521.

638 54. Falkowska E, Le KM, Ramos A, Doores KJ, Lee JH, Blattner C, Ramirez A, Derking R, van Gils
639 MJ, Liang CH, McBride R, von Bredow B, Shivatare SS, Wu CY, Chan-Hui PY, Liu Y, Feizi T,
640 Zwick MB, Koff WC, Seaman MS, Swiderek K, Moore JP, Evans D, Paulson JC, Wong CH, Ward
641 AB, Wilson IA, Sanders RW, Poignard P, Burton DR. 2014. Broadly neutralizing HIV antibodies

define a glycan-dependent epitope on the prefusion conformation of gp41 on cleaved envelope trimers. Immunity 40:657–668.

55. Blattner C, Lee JH, Sliepen K, Derking R, Falkowska E, delaPeña AT, Cupo A, Julien JP, vanGils M, Lee PS, Peng W, Paulson JC, Poignard P, Burton DR, Moore JP, Sanders RW, Wilson IA, Ward AB. 2014. Structural delineation of a quaternary, cleavage-dependent epitope at the gp41-gp120 interface on intact HIV-1 env trimers. Immunity 40:669–680.

56. Sattentau QJ, Moore JP. 1991. Conformational changes induced in the human immunodeficiency virus envelope glycoprotein by soluble CD4 binding. J Exp Med 174:407–415.

57. Hu X, Saha P, Chen X, Kim D, Devarasetty M, Varadarajan R, Jin MM. 2012. Cell surface assembly of HIV gp41 six-helix bundles for facile, quantitative measurements of hetero-oligomeric interactions. J Am Chem Soc 134:14642–14645.

58. Zhuang M, Wang W, De Feo CJ, Vassell R, Weiss CD. 2012. Trimeric, coiled-coil extension on peptide fusion inhibitor of HIV-1 influences selection of resistance pathways. J Biol Chem 287:8297–8309.

59. Thali M, Moore JP, Furman C, Charles M, Ho DD, Robinson J, Sodroski J. 1993. Characterization of conserved human immunodeficiency virus type 1 gp120 neutralization epitopes exposed upon gp120-CD4 binding. J Virol 67:3978–88.

60. Lewis GK, Fouts TR, Ibrahim S, Taylor BM, Salkar R, Guan Y, Kamin-Lewis R, DeVico AL. 2011. Identification and Characterization of an Immunogenic Hybrid Epitope Formed by both HIV gp120 and Human CD4 Proteins. J Virol 85:13097–13104.

61. Decker JM, Bibollet-Ruche F, Wei X, Wang S, Levy DN, Wang W, Delaporte E, Peeters M,

Derdeyn CA, Allen S, Hunter E, Saag MS, Hoxie JA, Hahn BH, Kwong PD, Robinson JE, Shaw GM. 2005. Antigenic conservation and immunogenicity of the HIV coreceptor binding site. J Exp Med 201:1407–1419.

62. Kaplan G, Roitburd-Berman A, Lewis GK, Gershoni JM. 2016. The range of CD4-bound conformations of HIV-1 gp120, as defined using conditional CD4-induced antibodies. J Virol 90:4481-4493.

63. Earl PL, Broder CC, Doms RW, Moss B. 1997. Epitope map of human immunodeficiency virus type 1 gp41 derived from 47 monoclonal antibodies produced by immunization with oligomeric envelope protein. J Virol 71:2674–2684.

64. Haim H, Strack B, Kassa A, Madani N, Wang L, Courter JR, Princiotto A, McGee K, Pacheco B, Seaman MS, Smith AB, Sodroski J. 2011. Contribution of intrinsic reactivity of the HIV-1 envelope glycoproteins to CD4-independent infection and global inhibitor sensitivity. PLoS Pathog 7:e1002101.

65. Pacheco B, Alsahafi N, Debbeche O, Prévost J, Ding S, Chapleau J-P, Herschhorn A, Madani N, Princiotto A, Melillo B, Gu C, Zeng X, Mao Y, Smith AB, Sodroski J, Finzi A. 2017. Residues in the gp41 Ectodomain Regulate HIV-1 Envelope Glycoprotein Conformational Transitions Induced by gp120-Directed Inhibitors. J Virol 91:e02219-16.

66. Depriest A, Phelan P, Martha Skerrett I. 2011. Tryptophan scanning mutagenesis of the first transmembrane domain of the innexin Shaking-B(Lethal). Biophys J 101:2408–2416.

67. Ananthaswamy N, Fang Q, AlSalmi W, Jain S, Chen Z, Klose T, Sun Y, Liu Y, Mahalingam M, Chand S, Tovanabutra S, Robb ML, Rossmann MG, Rao VB. 2019. A sequestered fusion peptide in

684 the structure of an HIV-1 transmitted founder envelope trimer. Nat Commun 10:873.

685 68. Kong R, Xu K, Zhou T, Acharya P, Lemmin T, Liu K, Ozorowski G, Soto C, Taft JD, Bailer RT,
686 Cale EM, Chen L, Choi CW, Chuang GY, Doria-Rose NA, Druz A, Georgiev IS, Gorman J, Huang
687 J, Joyce MG, Louder MK, Ma X, McKee K, O'Dell S, Pancera M, Yang Y, Blanchard SC, Mothes
688 W, Burton DR, Koff WC, Connors M, Ward AB, Kwong PD, Mascola JR. 2016. Fusion peptide of
689 HIV-1 as a site of vulnerability to neutralizing antibody. Science 352:828–833.

690 69. Ward AB, Wilson IA. 2017. The HIV-1 envelope glycoprotein structure: nailing down a moving
691 target. Immunol Rev 275:21-32.

692 70. Xu K, Acharya P, Kong R, Cheng C, Chuang GY, Liu K, Louder MK, O'Dell S, Rawi R, Sastry M,
693 Shen CH, Zhang B, Zhou T, Asokan M, Bailer RT, Chambers M, Chen X, Choi CW, Dandey VP,
694 Doria-Rose NA, Druz A, Eng ET, Farney SK, Foulds KE, Geng H, Georgiev IS, Gorman J, Hill
695 KR, Jafari AJ, Kwon YD, Lai YT, Lemmin T, McKee K, Ohr TY, Ou L, Peng D, Rowshan AP,
696 Sheng Z, Todd JP, Tsybovsky Y, Viox EG, Wang Y, Wei H, Yang Y, Zhou AF, Chen R, Yang L,
697 Scorpio DiG, McDermott AB, Shapiro L, Carragher B, Potter CS, Mascola JR, Kwong PD. 2018.
698 Epitope-based vaccine design yields fusion peptide-directed antibodies that neutralize diverse
699 strains of HIV-1. Nat Med 24:857–867.

700 71. Dingens AS, Acharya P, Haddox HK, Rawi R, Xu K, Chuang GY, Wei H, Zhang B, Mascola JR,
701 Carragher B, Potter CS, Overbaugh J, Kwong PD, Bloom JD. 2018. Complete functional mapping
702 of infection- and vaccine-elicited antibodies against the fusion peptide of HIV. PLoS Pathog
703 14:e1007159.

704 72. Dingens AS, Arenz D, Weight H, Overbaugh J, Bloom JD. 2019. An Antigenic Atlas of HIV-1
705 Escape from Broadly Neutralizing Antibodies Distinguishes Functional and Structural Epitopes.

Immunity 50:520–532.e3.

73. Sen J, Yan T, Wang J, Rong L, Tao L, Caffrey M. 2010. Alanine scanning mutagenesis of HIV-1 gp41 heptad repeat 1: insight into the gp120-gp41 interaction. Biochemistry 49:5057–5065.

74. Binley JM, Sanders RW, Clas B, Schuelke N, Master A, Guo Y, Kajumo F, Anselma DJ, Maddon PJ, Olson WC, Moore JP. 2000. A recombinant human immunodeficiency virus type 1 envelope glycoprotein complex stabilized by an intermolecular disulfide bond between the gp120 and gp41 subunits is an antigenic mimic of the trimeric virion-associated structure. J Virol 74:627–643.

75. Liu J, Wang S, Hoxie JA, LaBranche CC, Lu M. 2002. Mutations that destabilize the gp41 core are determinants for stabilizing the simian immunodeficiency virus-CPmac envelope glycoprotein complex. J Biol Chem 277:12891–12900.

76. Sanders RW, Vesanen M, Schuelke N, Master A, Schiffner L, Kalyanaraman R, Paluch M, Berkhout B, Maddon PJ, Olson WC, Lu M, Moore JP. 2002. Stabilization of the soluble, cleaved, trimeric form of the envelope glycoprotein complex of human immunodeficiency virus type 1. J Virol 76:8875–8889.

77. Liu Q, Acharya P, Dolan MA, Zhang P, Guzzo C, Lu J, Kwon A, Gururani D, Miao H, Bylund T, Chuang GY, Druz A, Zhou T, Rice WJ, Wigge C, Carragher B, Potter CS, Kwong PD, Lusso P. 2017. Quaternary contact in the initial interaction of CD4 with the HIV-1 envelope trimer. Nat Struct Mol Biol 24:370–378.

78. Lewis GK, Fouts TR, Ibrahim S, Taylor BM, Salkar R, Guan Y, Kamin-Lewis R, Robinson JE, DeVico AL. 2012. Identification and Characterization of an Immunogenic Hybrid Epitope Formed by both HIV gp120 and Human CD4 Proteins. J Virol 86:5410–5410.

79. Alsahafi N, Debbeche O, Sodroski J, Finzi A. 2015. Effects of the I559P gp41 change on the conformation and function of the human immunodeficiency virus (HIV-1) membrane envelope glycoprotein trimer. PLoS One 10:e0122111.

80. Bajaj K, Madhusudhan MS, Adkar B V., Chakrabarti P, Ramakrishnan C, Sali A, Varadarajan R. 2007. Stereochemical criteria for prediction of the effects of proline mutations on protein stability. PLoS Comput Biol 3:2465–2475.

81. Prajapati RS, Das M, Sreeramulu S, Sirajuddin M, Srinivasan S, Krishnamurthy V, Ranjani R, Ramakrishnan C, Varadarajan R. 2007. Thermodynamic effects of proline introduction on protein stability. Proteins Struct Funct Genet 66:480–491.

82. Indu S, Kumar ST, Thakurela S, Gupta M, Bhaskara RM, Ramakrishnan C, Varadarajan R. 2010. Disulfide conformation and design at helix N-termini. Proteins Struct Funct Bioinforma 78:1228–1242.

83. Schmidt T, Situ AJ, Ulmer TS. 2016. Structural and thermodynamic basis of proline-induced transmembrane complex stabilization. Sci Rep 6:29809.

84. Bhattacharyya S, Singh P, Rathore U, Purwar M, Wagner D, Arendt H, DeStefano J, LaBranche CC, Montefiori DC, Phogat S, Varadarajan R. 2013. Design of an Escherichia coli expressed HIV-1 gp120 fragment immunogen that binds to b12 and induces broad and potent neutralizing antibodies. J Biol Chem 288:9815–9825.

85. Li M, Gao F, Mascola JR, Stamatatos L, Polonis VR, Koutsoukos M, Voss G, Goepfert P, Gilbert P, Greene KM, Bilska M, Kothe DL, Salazar-Gonzalez JF, Wei X, Decker JM, Hahn BH, Montefiori DC. 2005. Human immunodeficiency virus type 1 env clones from acute and early

748 subtype B infections for standardized assessments of vaccine-elicited neutralizing antibodies. J
749 Virol 79:10108–10125.

750 86. Montefiori DC. 2005. Evaluating neutralizing antibodies against HIV, SIV, and SHIV in luciferase
751 reporter gene assays. Curr Protoc Immunol Chapter 12:Unit 12 11.

752 87. Rathore U, Saha P, Kesavardhana S, Kumar AA, Datta R, Devanarayanan S, Das R, Mascola JR,
753 Varadarajan R. 2017. Glycosylation of the core of the HIV-1 envelope subunit protein gp120 is not
754 required for native trimer formation or viral infectivity. J Biol Chem 292:10197–10219.

755 88. Kesavardhana S, Das R, Citron M, Datta R, Ecto L, Srilatha NS, DiStefano D, Swoyer R, Joyce JG,
756 Dutta S, LaBranche CC, Montefiori DC, Flynn JA, Varadarajan R. 2017. Structure-based Design of
757 Cyclically Permuted HIV-1 gp120 Trimers That Elicit Neutralizing Antibodies. J Biol Chem
758 292:278–291.

759

760

761 **Figure legends:**

762 **Figure 1:** Structure of BG505 SOSIP gp140. (A) Schematic showing different regions of gp41, dotted
763 lines representing the apparently disordered regions, (B) The left panel shows the crystal structure of
764 BG505 SOSIP gp140 (PDBID-4TVP) (40) showing the trimer axis (red vertical line). The right panel
765 shows a protomer of the BG505 SOSIP gp140 trimer, the stretch of residues with missing electron density
766 in most gp140 structures is shown as a dotted line, (C)Post-fusion structure (PDB ID 1AIK). N- heptad
767 repeat (NHR) in green and C- heptad repeat (CHR) in blue, left and right panels show views from side and
768 bottom respectively, NHR and CHR form a six-helix bundle structure during viral fusion, where NHR

forms a parallel trimeric coiled-coil and CHR's bind anti-parallely to the outside of this NHR coiled coil. The N and C termini of one protomer of NHR and CHR are labelled in pink and red color respectively.

Figure 2: Surface expression of Asp mutants. Cell surface expression levels were detected by 2G12 antibody binding, the 2G12 binding ratio is calculated with respect to the wild- type. HEK 293T cells were transfected with constructs. After 48 hours, the transfected cells were harvested and probed with 2G12 as primary antibody and anti-human PE to quantitate cell surface expression. All the mutants are normalized to wild type where wild type ratio is 1. The vertical bars represent the mean ratio value for each mutant along with standard deviation from three independent experiments analyzed using an unpaired t-test (*, P< 0.05; **, P< 0.01; ***, P< 0.001; **** P< 0.0001; ns, non- significant, p>0.05).

Figure 3: Conformational integrity of mutants. This is determined by measuring the ratio of the binding of the neutralizing antibody b12 to the binding of non-neutralizing b6 to HIV-1 Env displayed on HEK293T cells. HEK 293T cells were transfected with constructs. After 48 hours, the transfected cells were harvested and probed with 2G12 as primary antibody for expression and anti-human PE as secondary antibody All the mutant values are normalized to wild type where the wild type ratio is 1. The vertical bars represent the mean value for each mutant along with standard deviation from three independent experiments analyzed using unpaired t-test (*, P < 0.05; **, P < 0.01; ***, P < 0.001; **** P < 0.0001; ns, non- significant, p>0.05).

Figure 4: Effect of mutations on sCD4 induced shedding of gp120, as determined by FACS. The mutant proteins were expressed on the cell surface. Cells were incubated with sCD4 to induce gp120 shedding. The cells were washed once with FACS buffer and the gp120 remaining on the cell surface was quantified by staining cells with 2G12 at a concentration of 10 μg/ml. The ratio of MFI's from sCD4 treated and

untreated cells for each mutant is shown for A) mutants that did not prevent shedding, (B) mutants that prevented shedding. V570D was taken as a positive control as it is known to prevent shedding (28).

Figure 5: Probing/ binding of mutant Env's to 17b, 19e and D49 following incubation with sCD4. All the constructs were transfected into HEK293T cells. After 48 hours, transfected cells were harvested and incubated with sCD4 for 2 hours and washed to remove shed gp120 and incubated with A) 17b, B) 19e or C) D49 for one hour and washed and probed for antibody binding with phycoerythrin labeled secondary antibody using FACS. A second set of cells was similarly probed for antibody binding without sCD4 incubation. The MFI ratio of (sCD4 treated)/ untreated) was calculated.

Figure 6: Pseudoviral infectivity in TZMbl cells for aspartate mutants in the fusion peptide and N-heptad repeat regions of gp41. Equivalent p24 levels of virions were used to measure infectivity.

Figure 7: Structural information from post fusion structure: Residues mapped on post fusion structure (PDB ID: 1AIK). A) Residues that prevent sCD4 gp120 shedding, (B) Residues that do not prevent gp120 shedding, (C) N-heptad repeat (NHR: green) and C-heptad repeat (CHR: blue) arranged in coiled-coil fashion. Residues that prevent gp120 shedding mainly lie between the NHR: NHR interface at positions "a" and "d" and at NHR: CHR interface positions "e" and "g". There are also residues that lie in exposed positions at the NHR that prevent shedding (Table 1, and 2).

Figure 8: Web logo showing residue conservation for the disordered stretch of residue. Residues that prevent gp120 shedding are not more conserved than residues that do not prevent gp120 shedding. The residues highlighted with * prevent sCD4 induced gp120 shedding.

Figure 9: Cleavage efficiency of mutants expressed on the cell surface. Cleavage was monitored by PGT151 binding. Most mutants showed similar cleavage efficiency to the WT.

811 **Figure 10:** Conformational integrity and sCD4 induced gp120 shedding of Clade C Env 4-2 J.41
812 expressed on the surface of HEK 293T cells. (A) Mutants of Clade C Env were transfected into HEK
813 293T cell and probed for binding to VRC01 and F105 MAbs. (B) Transfected cells were incubated with
814 sCD4 to induce gp120 shedding (46, 47).

815

816

817 ..

818

819

820

821

822

823

824

825

826

827

Figure 1

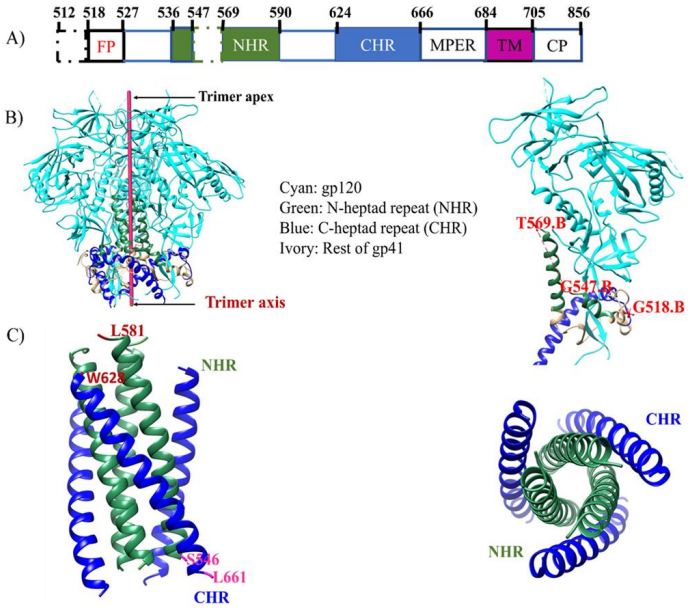

Figure 2

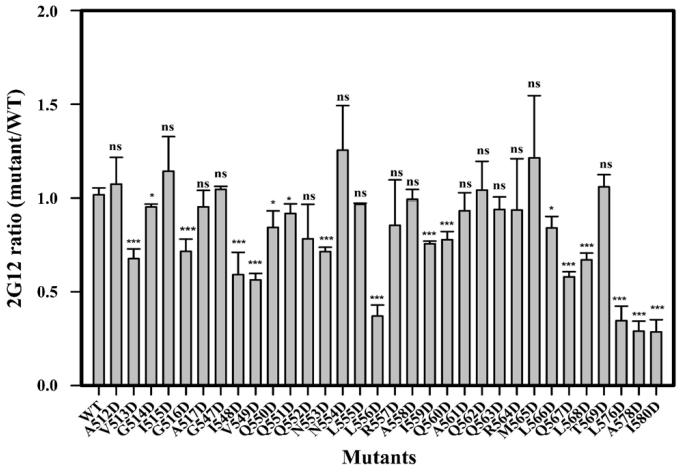

Figure 3

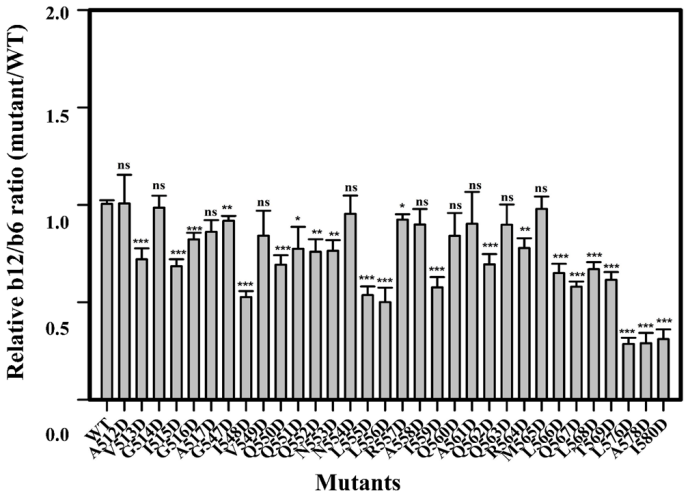

Figure 4

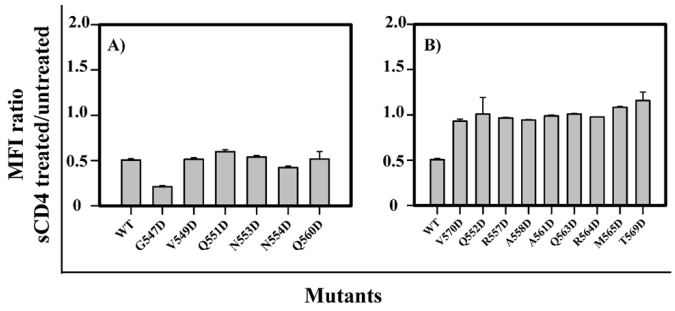

Figure 5

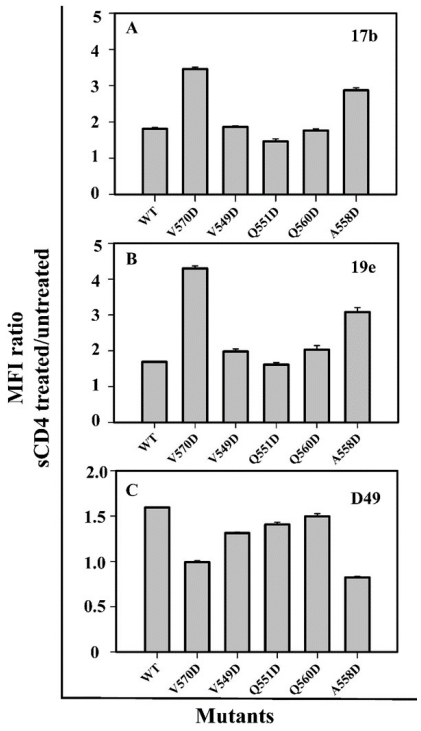

Figure 6

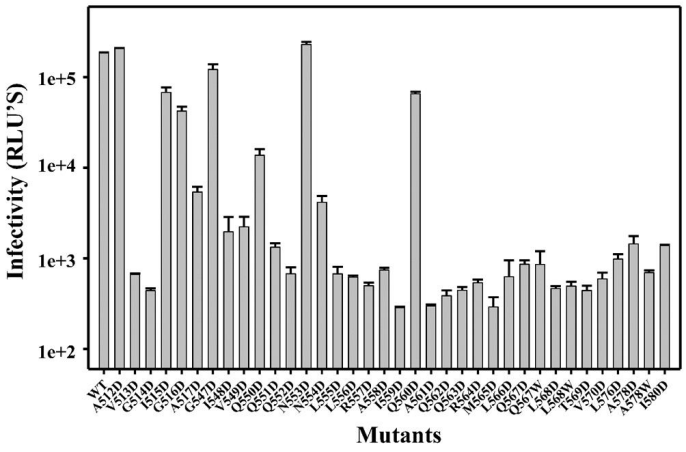

Figure 7

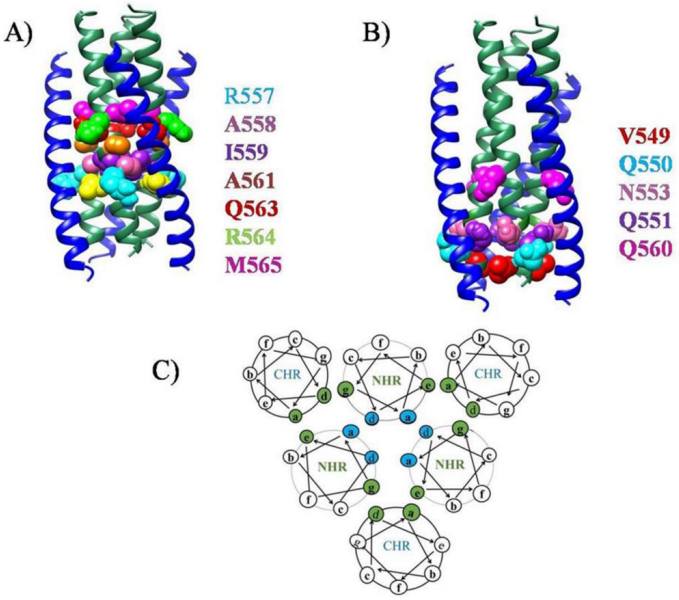

Figure 8

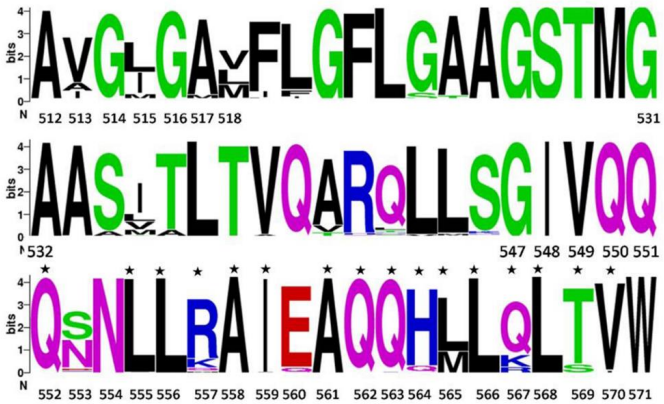

Figure 9

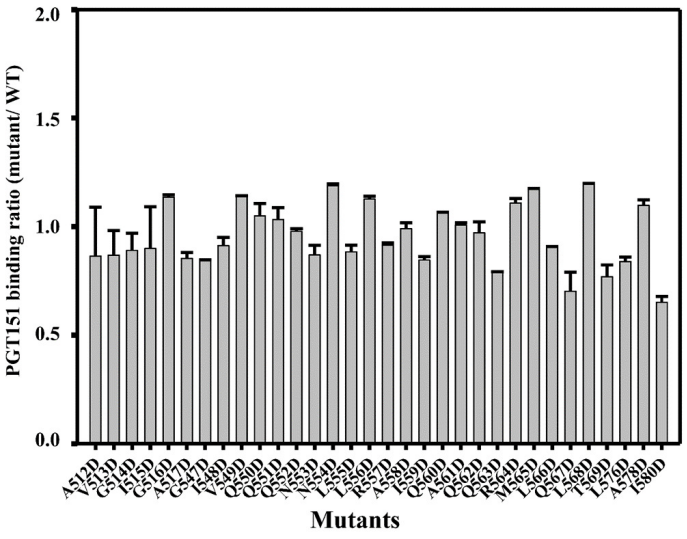

Figure 10

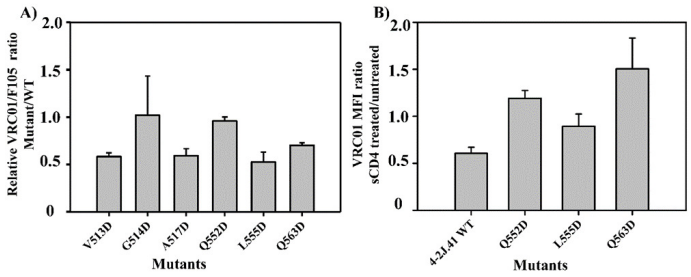

TABLES:

Table 1: Summary of the surface expression and antibody binding data for Asp mutants. The surface expression and b12/b6 ratio shown are from three independent experiment along with standard deviation (Mean± SD). The position of all mutants in the helical wheel diagram of the NHR in the post-fusion 6HB is also shown.

Residue no	Mutation	Position in helical wheel	Surface expression (Mean± SD)	b12/ b6 ratio (Mean ± SD)	Alanine scanning result[a,b]	Infectivity of Asp mutant
WT	-	-	1.02 ± 0.04	1.01 ± 0.02		
512	A512D	-	1.07 ± 0.14	1.01 ± 0.15		110± 3.0%
513	V513D	-	0.68 ± 0.05	0.73 ± 0.07		Non-infective
514	G514D	-	0.95 ± 0.02	0.99 ± 0.06		Non-infective
515	I515D	-	1.14 ± 0.18	0.69 ± 0.04		36.65± 7.2 %
516	G516D	-	0.72 ± 0.07	0.82 ± 0.03		23.04± 3.9%
517	A517D	-	0.95 ± 0.09	0.86 ± 0.06		3.4±0.5890
547	G547D	c	1.05 ± 0.02	0.92 ± 0.02	Wt like[b]	65.34±12.13%
548	I548D	d	0.59 ± 0.12	0.53 ± 0.03	Wt like[b]	~2%
549	V549D	e	0.56 ± 0.03	0.84 ± 0.13	Wt like[b]	~1%
550	Q550D	f	0.84 ± 0.09	0.69 ± 0.05	Wt like[b]	7.84±1.73%
551	Q551D	g	0.92 ± 0.05	0.77 ± 0.11	Wt like[b]	Non-infective
552	Q552D	a	0.78 ± 0.18	0.76 ± 0.06	nffolding[a]and Imp association[b]	Non-infective
553	N553D	b	0.71 ± 0.02	0.76 ± 0.05	Reduced cleavage[b]	122.93±11.8%
554	N554D	c	1.26 ± 0.24	0.95 ± 0.09	Wt like[b]	2.7±0.53%
555	L555D	d	0.97 ± 0.01	0.54 ± 0.02	Reduced cleavage[b]	Non-infective
556	L556D	e	0.37 ± 0.06	0.47 ± 0.07	Imp folding and association[a, b]	Non-infective
557	R557D	f	0.85 ± 0.24	0.92 ± 0.03	Wt like[b]	Non-infective
558	A558D	g	0.99 ± 0.05	0.9 ± 0.08	Imp association[b]	Non-infective
559	I559D	a	0.76 ± 0.01	0.58 ± 0.05	Imp association[b]	Non-infective
560	Q560D	b	0.78 ± 0.04	0.84 ± 0.12	nffolding[a]	35.4±2.68%
561	A561D	c	0.93 ± 0.1	0.9 ± 0.16	Impaired association[b]	Non-infective
562	Q562D	d	1.04 ± 0.15	0.69 ± 0.05	Imp folding[a]	Non-infective
563	Q563D	e	0.94 ± 0.07	0.9 ± 0.1	Wt like[b]	Non-infective
564	R564D	f	0.94 ± 0.27	0.78 ± 0.05	Wt like[b]	Non-infective
565	M565D	g	1.21 ± 0.33	0.98 ± 0.06	Impaired	Non-infective

					processing[b]	
566	L566D	a	0.84 ± 0.06	0.65 ± 0.05	Impaired association and processing[b]	Non-infective
567	Q567D	b	0.58 ± 0.03	0.58 ± 0.03	Impaired association and processing[b]	Non-infective
	Q567W	b	0.93±0.044	0.44 ± 0.104		Non-infective
568	L568D	c	0.67 ± 0.04	0.67 ± 0.04	Impaired association[b]	Non-infective
	L568W	c	0.89 ± 0.044	0.75±0.04		Non-infective
569	T569D	d	1.06 ± 0.06	0.62 ± 0.04	nf association[a]	Non-infective
576	L576D	d	0.35 ± 0.08	0.29 ± 0.05	nf association[a], impaired processing[b]	Non-infective
578	A578D	f	0.26 ± 0.08	0.29±0.05		Non-infective
	A578W	f	0.93±0.03	0.86±0.06		Non-infective
580	I580D	d	0.29 ± 0.06	0.31 ± 0.05	nf association [a, b]	Non-infective

[a] Ala scanning mutants (73), based on viral entry that have impaired (Imp) folding (5-40% entry and have < 25% gp41), non-functional (nf) folding (<5% entry and have < 25% gp41) and non-functional (nf) association (<5% entry with gp120/gp41 ratio >0.5) respectively (73) [b] (65).

Table 2: Comparative summary of accessibilities of mutants in Cryo-EM prefusion structure (PDB ID-5FUU) and post-fusion structures of gp41 (PDB ID- 1AIK) and effect of Asp mutants on gp120 shedding. The Cryo-EM structure is in complex with PGT 151. The MAb binds asymmetrically to D and F chains of gp41, on account of this all the three gp140 interfaces are not equivalent. Consequently, the unliganded protomer (1) is found to be conformationally variable in comparison to the liganded protomers as is clearly evident from the accessibility values. The N-heptad repeat residues lie at different position in the helical wheel in the post-fusion conformation (PDB 1AIK) and have different % accessibilities. There is no clear correlation between residue accessibility in the post-fusion structure and ability to prevent sCD4 induced shedding.

Residue no	Position in helical wheel 6-helix bundle	Residue	Prefusion accessibilities in 5FUU (%)			Post fusion accessibilities in 1AIK (%)	Prevention of sCD4 induced gp120 shedding
			Protomer1	Protomer 2	Protomer 3		
547	c	GLY	17.5	77.9	80.9	13.1	No
548	d	ILE	80.7	28.8	50.6	10.9	No
549	e	VAL	43.3	57.2	62.4	6.1	No
550	f	GLN	24.4	61.5	73.5	50.1	No
551	g	GLN	61.4	94.1	57.4	0	No
552	a	GLN	66.7	38.3	40.7	0	Yes
553	b	ASN	17.8	98.5	57.8	47.3	No
554	c	ASN	45.8	83.2	80	0	No
555	d	LEU	74	9.1	19.1	0.1	Yes
556	e	LEU	17.7	36.6	28.1	4.4	Yes
557	f	ARG	12	95.5	73.1	49.1	Yes
558	g	ALA	89.3	17.4	10.9	0.8	Yes
559	a	ILE	48	17.2	32.3	0.2	Yes
560	b	GLU	22.8	35.7	41.7	27.7	No
561	c	ALA	53.2	56.2	52.9	3.2	Yes
562	d	GLN	76.2	8.5	5.4	1	Yes
563	e	GLN	15.4	19.5	15.5	1	Yes
564	f	ARG	19.7	31.9	30.4	54.6	Yes
565	g	MET	55.3	47.2	47.9	0.1	Yes
566	a	LEU	16	3.6	5.7	1.4	Yes

567	b	GLN	60.5	43.5	5	37.5	Yes
568	c	LEU	23.8	21.1	38.5	18	No
569	d	THR	24.3	56	39.9	0.9	Yes
570	e	VAL	2	39.8	19.9	3.2	Yes